LETTER

Stacked Silicon Nanowires with Improved Field Enhancement Factor

Yu-Fen Tzeng,[†] Hung-Chi Wu,[†] Pei-Sun Sheng,[§] Nyan-Hwa Tai,[†] Hsin Tien Chiu,[§] Chi Young Lee,[†,‡] and I-Nan Lin*[,⊥]

Department of Materials Science and Engineering and Center of Nanotechnology, Materials Science, and Microsystem, National Tsing Hua University, Hsinchu, Taiwan, Department of Applied Chemistry, National Chiao Tung University, Hsinchu, Taiwan, and Department of Physics, Tamkang University, Tamsui, Taiwan

ABSTRACT This work describes newly structured stacked silicon nanowires (s-SiNWs), consisting of nanosized silicon wires on top of silicon microrods (SiMRs) and exhibiting pronouncedly superior electron field emission (EFE) characteristics to the conventional SiNWs, by using a two-step electroless metal deposition process. Experimental results indicate that for these s-SiNWs, the electrostatic "screen effect" is markedly suppressed and the field enhancement factor (β-value) is significantly increased ($(\beta)_{\text{s-SiNWs}} = 2533$). Additionally, the turn-on field (E_0) for triggering the EFE process is reduced to a level comparable with that of carbon nanotubes, viz. $(E_0)_{\text{s-SiNWs}} = 2.0$ V/μm. This simple and robust modified electroless metal deposition approach does not require either a high temperature or an expensive photolithographic process and possesses great potential for applications.

KEYWORDS: silicon nanowires • electroless metal deposition • electron field emission.

INTRODUCTION

One-dimensional nanomaterials, including nanotubes and nanowires, have attracted increasing attention owing to their novel physical properties and a diverse array of potential nanodevice-related applications (1−3). Among the vacuum microelectronic devices, applications for which field emitters are of great technological importance include field emission displays, microwave devices, and X-ray sources (4). Superior to other nanowires in their compatibility with Si materials, Si nanowires (SiNWs) are highly promising for integration with Si devices to form active electron field emitters. Aligned single-crystalline Si nanoemitters have been fabricated by laser ablation (5) and self-masked chemical etching (6), whereas randomly oriented SiNWs have been fabricated by vapor−liquid−vapor growth (VLS) (7−10). However, a relatively large electrical field is still required to turn on electron field emissions (EFE) because of either the large-sized pyramidal Si tips or the imperfect crystallinity of the wormlike SiNWs. Decreasing the turn-on field for such one-dimensional nanomaterials is thus urgently required (11, 12). Moreover, practical applications require Si-nanowires with high rigidity that can withstand device fabrication processes.

This work presents a modified electroless metal deposition (EMD) procedure for fabricating stacked silicon nanowires (s-SiNWs) with enhanced EFE properties. Well-dispersed silicon microrods (SiMRs) are fabricated using the conventional EMD process (13, 14), followed by Galvanic etching. The s-SiNWs thus obtained possess EFE properties that are superior to those of conventional silicon nanowires and are comparable with those of carbon nanotubes (CNTs).

EXPERIMENTAL SECTION

In the conventional EMD process for fabricating silicon nanowires, (100) or (111) Si substrates containing nanosized Au clusters were etched in aqueous $AgNO_3$ ($AgNO_3$ 0.103 M and HF 27.586 M, etchant I) for 30 min (14). In contrast with a one-step etching procedure for synthesizing the vertically aligned SiNWs, We fabricated the newly structured SiNWs by a two-step process, including anisotropic etching and self-Galvanic etching processes. In this process, the cleaned (111) Si-substrates were initially immersed directly in a silver-containing solution ($AgNO_3$ 0.010 M and HF 4.60 M) for an extremely short period (15 s) to produce large Ag islands (100−150 nm in size) on Si substrates. Substrates containing large Ag-islands were cleaned and then immersed in an etchant comprising H_2O_2 0.020 M and HF 5.000 M (etchant II_a) in ethanol for 30 min to form silicon microrods (SiMRs). The SiMRs were then etched in EMD etching solution ($AgNO_3$ 0.043 M and HF 15.623 M, etchant II_b) again for 30 min, yielding sculptured SiMRs with crosswise silicon nanowire bundles, which were designated as stacked SiNWs (s-SiNWs). Notably, in the anisotropic etching process for fabricating the SiMRs, the etchant chemicals are not critical, but in the sharpening process, the $AgNO_3$ content in the EMD etchant must be controlled tightly such that the Ag nanodots with a size of around a few nanometers can form on the surface of the SiMRs before anisotropic Galvanic etching.

The morphologies and the crystal structure of the SiNWs were examined using scanning electron microscopy (SEM, JEOL JSM-6500F) and transmission electron microscopy (TEM, JEOL JEM-4000EX), respectively. The EFE properties of the SiNWs were determined using a parallel plate setup, in which the sample-to-anode distance was adjusted using a micrometer. The current density-electric field ($J-E$) characteristics were determined using an electrometer (Keithley 237) under 1×10^{-6} Torr. The

* Corresponding author. E-mail:inanlin@mail.tku.edu.tw; Tel: +886-2-2626890.
Received for review August 6, 2009 and accepted December 14, 2009
† Department of Materials Science and Engineering, National Tsing Hua University.
‡ Center of Nanotechnology, Materials Science, and Microsystem, National Tsing Hua University.
§ National Chiao Tung University.
⊥ Tamkang University.
DOI: 10.1021/am900490m
© 2010 American Chemical Society

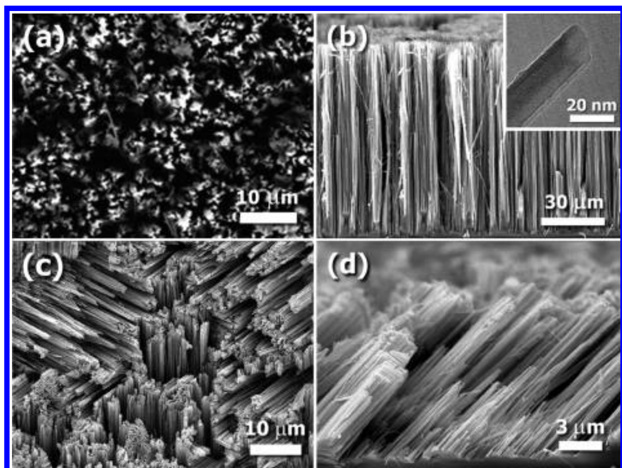

FIGURE 1. (a) Top and (b) side view SEM micrograph of SiNWs(100), which were prepared using (100) Si substrates, and the (c) top and (d) side view SEM micrograph of SiNWs(111), which were prepared using (111) Si substrates. The SiNWs were etched by conventional EMD process in aqueous $AgNO_3$ ($AgNO_3$ 0.103 M and HF 27.586 M).

EFE characteristics were explained using a Fowler−Nordheim (F−N) model (15, 16)

$$J = (A\beta^2E^2/\phi)\exp(-B\phi^{3/2}/\beta E), \quad (1)$$

where J denotes the current density; β and E represent the field enhancement factor and the applied field strength, respectively, and ϕ is the work function of the emitting materials. A and B are constants ($A = -1.56 \times 10^{-10}$ AV^{-2} eV and $B = 6.83 \times 10^3$ VeV$^{-3/2}$ µm^{-1}). The turn-on field (E_0) was designated as the intercept of the straight lines extrapolated from the low-field and high-field segments of the F−N plots. The β of these SiNWs was determined from the slope of the Fowler−Nordheim plots (slope $= B(\phi^{3/2}/\beta)$).

RESULTS AND DISCUSSION

SEM micrographs a and b in in Figure 1 illustrate the top and side views of SiNWs fabricated using a (100)-oriented Si substrate, the SiNWs(100), by the conventional anisotropic etching procedure (13, 14). The inset in Figure 1b displays the TEM micrograph of the SiNWs(100), revealing that they are extremely small in size and roughly 50 nanometers in diameter. All of the SiNWs(100) are of the same height, forming bundles. Moreover, micrographs c and d in Figure 1 display the SEM morphology of the SiNWs produced by the same etching process using (111) Si substrates, the SiNWs(111). The characteristics of the SiNWs are compared by evaluating the electron field emission behavior of these SiNWs. Figure 2 and its inset display the $J-E$ curves and the corresponding Fowler-Nordheim plots of the SiNWs(100), respectively. The solid curves are fitted with each other using the F−N model (15, 16), indicating that the $J-E$ curves fit F−N model very well, i.e., these EFE properties can be explained very well using the F−N theory (eq 1). Table 1 lists the important EFE parameters extracted from the $J-E$ curves. According to the $J-E$ curve in Figure 2 (solid squares symbols), the EFE of these SiNWs(100) can be turned on at $(E_0)_{SiNWs(100)} = 8.6$ V/µm, yielding an EFE current density of $(J_e)_{SiNWs(100)} = 4.7$ µA/cm^2 in an applied field of 12 V/µm. In

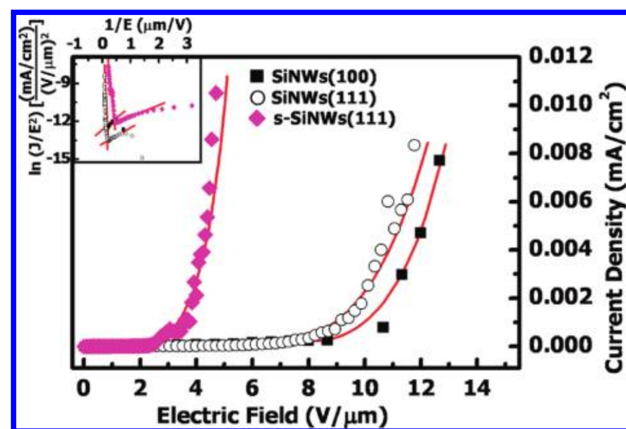

FIGURE 2. Electron field emission properties, current density, and electric field ($J-E$) curves, and the corresponding Fowler−Nordheim plots for the SiNWs.

Table 1. Electron Field Emission Properties of Conventional SiNWs and Stacked SiNWs (s-SiNWs)[a]

	SiNWs(100)	SiMRs(111)	s-SiNWs(111)
J_e (µA/cm^2) at Ea	4.7 (12.0)	8.3 (12.0)	2.1 (4.0)
E_0 (V/µm)	8.6	4.0	2.0
β	440	1147	2533

[a] J_e: the electron field emission current density achieved at applied field E_a, which is specified in parentheses. E_0: the turn-on field derived from Fowler−Nordheim plots, as the interceptions of straight lines extrapolated from the low-field and high-field segments of the F−N plots. β: the field enhancement factor deduced from $J-E$ curves using the F−N model (the theoretical field enhancement factor estimated for an individual SiNW with 60 nm in diameter and 90 µm in height is $\beta_0 = 3000$).

contrast, the $J-E$ curve in Figure 2 (open circle symbols) indicates that the EFE process for SiNWs(111) nanotips can be turned on at $(E_0)_{SiNWs(111)} = 4.0$ V/µm, yielding an EFE current density of $(J_e)_{SiNWs(111)} = 8.3$ µA/cm^2 in an applied field of 12 V/µm.

By assuming that the work function (ϕ) of SiNWs is the same as that of bulk Si materials (17), $\phi_{Si} = 4.1$ eV, we estimated the β values of these SiNWs from the slope of the F−N plots (inset, Figure 2), resulting in $\beta_{SiNWs} = 440$, and 1147 for SiNWs(100) and SiNWs(111), respectively. Obviously, the superior EFE properties for SiNWs(111), in contrast with those for SiNWs(100), arise from the larger field enhancement factor for the SiNWs(111). It should be noted that the arrangement of the nanostructures alters pronouncedly the EFE behavior of the nanostructure assembly has been modeled using tunneling theory (18). By means of numerical computation, it was observed that when many nanostructures (like CNTs) were brought together, a neighborhood screening effect appears and the local field on the tip of nanostructures decreases sharply with distance between the nearest neighbors. A phenomenological formula was proposed

$$F = \beta(V/d) \text{ with } \beta = 1 + s(d/r_0) \quad (2)$$

where F is the local field on the tip of nanostructure, β is the field enhancement factor, V is the applied electrical potential,

d and r_0 are anode-to-cathode spacing and radius of curvature for the CNTs, respectively; s is the screening effect parameters, whose range is between 0 for very densely arranged CNTs and 1 for a single CNTs. The d/r_0 is usually of the order of 1000 for CNTs.

Apparently, the dense packing of the equal-height Si nanowires incurs a large "screening effect" for the SiNWs(100), that significantly reduced the β-factor. Conversely, the Si-nanowires in SiNWs(111) are inclined to each other the emitter tip density in which the markedly lowered, subsequently increasing the β-factor. Restated, the β-value largely influences the EFE behavior for these SiNWs. The field-enhanced factor for an isolated Si-nanowire, with $d = 90\ \mu$m and $r = 60$ nm, located in a parallel-plates electrical field can be calculated theoretically as $\beta_0 = 3000$ (19). This finding suggests that the field enhancement factor of these SiNWs is significantly lower than that of the theoretically predicted values (β_0). Restated, the SiNWs shown in Figure 1 are too closely packed together, subsequently incurring a large "screening effect".

Theoretical calculation using "the model of a floating top segment" (20) or in the framework of "quantum theory of many electrons" (21), as well as computation using commercial package (Simion 3D 7.0) (22) for CNTs, concluded that the applied external field is strongly screened when the spacing between CNTs is shorter than the length of CNTs. The optimal spacing is two to three times of CNT length for maximizing the field enhancement factor resulted from high aspect ratio of CNTs. Although the calculations/simulations were performed for CNTs, the same behavior is expected for SiNWs, as the calculations/simulations were mainly based on the geometry of the field emitting nanostructures and the nature of materials is immaterial. Therefore, to suppress the "screen effect(s)" so as to enhance the β-factor for EFE process, increasing the spacing between SiNWs is necessary.

The attempt to reduce the packing density of the SiNWs using Si-substrates that contain scarcely distributed Au nanodots in EMD process is unsuccessful because the widely separated SiNWs are too fragile to survive the subsequent cleaning process. A modified EMD process, capable of lowering the packing density of SiNWs while maintaining the rigidity of the nanowires, is thus warranted. The stratagem is to fabricate well-separated SiMRs and then sharpen the silicon rods in an EMD process. It should be noted that, for the weak etchants ($AgNO_3$ 0.103 M and HF 27.586 M, etchant I) used, the Galvanic etching process always took place along the [100] orientation, leading to the [100]SiNWs. To modify such a behavior, a stronger etchant, capable of etching the Si materials vertically along the substrate normal without the restricting of the [100] substrate orientation, is apparently required. The etchant comprising H_2O_2 0.020 M & HF 5.000 M in ethanol (etchant II_a) is apparently a good choice because H_2O_2 is a strong oxidation agent. Figure 3a displays the top view SEM image of SiMRs formed on (111) Si substrates by etching of Si-substrates using etchant II_a, containing uniformly distributed large Ag clusters (inset,

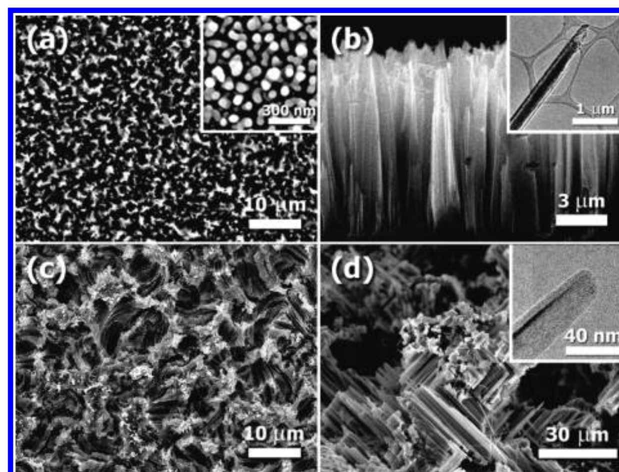

FIGURE 3. (a) Top and (b) side view SEM micrograph of SiMRs, which were prepared by etching (111)Si-substrates in $AgNO_3$ 0.01 M and HF 4.6 M; and the (c) top and (d) side view SEM micrograph of s-SiNWs, which were prepared on SiMRs, by EMD process in aqueous $AgNO_3$ ($AgNO_3$ 0.043 M and HF 15.623 M).

Figure 3a), for 30 min. Figure 3b illustrates the side view SEM images of SiMRs, indicating that the SiMRs are approximately 500 nm in diameter and of 9 μm in height. Ag nanodots are then formed on SiMRs to trigger the self-aligned Galvanic etching process, using etahant II_b, from both the top surfaces and the side walls of SiMRs simultaneously, subsequently yielding sculptured SiMRs with crosswise silicon nanowire bundles which are designated as stacked-SiNWs. The SEM micrographs c and d in Figure 3 illustrate the homogenized interlacing of inclined stacked silicon networks. The s-SiNWs are 50 μm in height, and the mean distance between them is of a similar order of magnitude. Figure 3d shows some nanosized silicon nanowires on top of s-SiNWs.

The $J-E$ curve in Figure 2 (closed diamond symbols) reveals that the EFE of the SiNWs has been pronounced enhanced due to these newly designed process, i.e., the EFE of s-SiNWs can be turned on at significantly smaller electric fields, $(E_0)_{\text{s-SiNWs}} = 2.0$ V/μm, yielding a considerably larger EFE current density, $(J_e)_{\text{s-SiNWs}} = 2.1\ \mu$A/cm^2, in an applied field of 4.0 V/μm, which are markedly better than those of SiNWs(100) or SiNWs(111). The emission current appears to be attributed largely to the SiNWs grown on the top surface of the SiMRs. The β-value of these s-SiNWs is estimated from the corresponding F−N plots as $(\beta)_{\text{s-SiNWs}} = 2533$, which is markedly larger than those of SiNWs(100) and SiNWs(111), as shown in Table 1. The above results clearly demonstrate the advantage of the modified EMD process in enhancing the EFE properties of Si-emitters. Notably, the turn-on fields attainable for s-SiNWs are significantly lower than the E_0 value attainable for silicon tips prepared by the other chemical vapor deposition (CVD) process (5−10), which are summarized in Table 2. One possible explanation for such a result is that most of the CVD-grown SiNWs are entangled (see the Supporting Information), indicating that they contain a large proportion of

LETTER

LETTER

Table 2. Comparison on the Characteristics of Typical SiNWs and Si Tips (5−10)

	ref						
	5	6	7	8	9	10	this study
synthesis technique[a]	LA	SE	CVD	CVD	CVD	CVD	S. E.
processing temp. (°C)	rt	rt	480	1200	511	450	r. t.
morphologies[b]	V	V	R	R	R	R	V
dimensions (nm)	8	1000	100	5−10	60	25−50	20−40
E_0 (V/μm)	p-Si 1−2 n-Si 4−5	25.0	5.5	6.3	27.0	7.4	2.1

[a] CVD: chemical vapor deposition. LA, laser ablation; SE, self-masked etching process. [b] R, randomly oriented SiNWs. V, vertically aligned pyramidal Si-tips. [c] E_0, turn-on field.

defects, whereas the SiNWs formed by the aforementioned modified EMD process are single-crystalline with very few defects.

Importantly, the multistep EMD procedure for synthesizing s-SiNWs proceeds at room temperature and does not involve expensive photolithographic process. Although the EFE properties of s-SiNWs are still slightly inferior to those of CNTs (23, 24), which can be turned on at $(E_0)_{\mathrm{CNTs}} = 1.9-2.1$ V/μm, attaingin $(J_e)_{\mathrm{CNTs}} = 10$ μA/cm^2 at 1.9 V/μm, the pattern of the emission sites on the Si wafers for fabricating s-SiNWs is markedly simpler than that for growing CNTs. Reliable electron field emitters with EFE properties comparable with that of CNTs can be obtained once the s-SiNWs are coated with low-work-function materials, e.g., LaB_6, Cs-metal, or ultrananocrystalline diamond (UNCD) films. More importantly, the multistep EMD process is much more robust and reproducible than that of the CVD process in terms of growing CNTs. The s-SiNWs fabricated by the modified EMD process can serve as a valuable reference for synthesizing practical device applications.

In summary, Si-nanowires (SiNWs) with an enhanced field enhancement factor are fabricated by carefully modifying the etching conditions in the electroless metal deposition (EMD) process. The conventional EMD process anisotropically etches Au nanodot coated Si that yields vertically aligned SiNWs with a large "screening effect". The two-step EMD procedure, in which Si-microrods (SiMRs) form before Galvanic etching, yields stacked SiNWs with interlacing SiNWs. The electrostatic "screening effect" for the s-SiNWs is markedly suppressed to the extent that the β-value of s-SiNWs is substantially increased to $(\beta)_{\mathrm{s\text{-}SiNWs}} = 2533$. Furthermore, the turn-on field for triggering the EFE process for these s-SiNWs is lowered to a level comparable with that of CNTs, viz. $(E_0)_{\mathrm{s\text{-}SiNWs}} = 2.0$ V/μm.

Acknowledgment. The authors thank National Science Council, ROC, for the support of this research through Project NSC 95-2113-M-007-030 and NSC 96-2112-M032-011-MY3.

Supporting Information Available: SEM image of the CVD-grown SiNWs (PDF). This material is available free of charge via the Internet at http://pubs.acs.org.

REFERENCES AND NOTES

(1) Teo, B. K.; Sun, X. H. *Chem. Rev.* **2007**, *107*, 1454.
(2) Chaudhry, A.; Ramamurthi, V.; Fong, E.; Islam, M. S. *Nano Lett.* **2007**, *7*, 1536.
(3) Tsutsumi, T.; Ishii, K.; Hiroshima, H.; Kanemaru, S.; Suzuki, E.; Tomizawa, K. *J. Appl. Phys.* **2002**, *41*, 4419.
(4) Chattopadhyay, S.; Chen, L. C.; Chen, K. H. *Crit. Rev. Solid State Mater. Sci.* **2006**, *31*, 15.
(5) Karabutov, A. V.; Frolov, V. D.; Loubnin, E. N.; Simakin, A. V.; Shafeev, G. A. *Appl. Phys. A: Mater. Sci. Process.* **2003**, *76*, 413.
(6) Fung, Y. M.; Cheung, W. Y.; Wilson, I. H.; Chen, D.; Xu, J. B.; Wong, S. P.; Kwok, R. W. M. *J. Vac. Sci. Technol., B* **2001**, *19*, 884.
(7) Zeng, B.; Xiong, G.; Chen, S.; Jo, S. H.; Wang, W. Z.; Wang, D. Z.; Ren, Z. F. *Appl. Phys. Lett.* **2006**, *88*, 213108.
(8) Chueh, Y. L.; Chou, L. J.; Cheng, S. L.; He, J. H.; Wu, W. W.; Chen, L. J. *Appl. Phys. Lett.* **2005**, *86*, 133112.
(9) Riccitelli, R.; Carlo, A. D.; Fiori, A.; Orlanducci, S.; Terranova, M. L.; Santoni, A.; Fantoni, R.; Rufoloni, A.; Villacorta, F. J. *J. Appl. Phys.* **2007**, *102*, 054906.
(10) McClain, D.; Solanki, R.; Dong, L.; Jiao, J. *J. Vac. Sci. Technol., B* **2006**, *24*, 20.
(11) Johnson, S.; Markwitz, A.; Rudolphi, M.; Baumann, H.; Oei, S. P.; Teo, K. B. K.; Milne, W. I. *Appl. Phys. Lett.* **2004**, *85*, 3277.
(12) Zeng, B.; Xiong, G.; Chen, S.; Wang, W.; Wang, D. Z.; Ren, Z. F. *Appl. Phys. Lett.* **2007**, *90*, 033112.
(13) Peng, K. Q.; Yang, Y. J.; Gao, S. P.; Zhu, J. *Adv. Mater.* **2002**, *14*, 1164.
(14) Tzeng, Y. F.; Lee, Y. C.; Liu, K. H.; Lin, S. J.; Lin, I. N.; Lee, C. Y.; Chiu, H. T. *Nanotechnology* **2007**, *18*, 435703.
(15) Fowler, R. H.; Nordheim, L. W. *Proc. R. Soc. London, Ser. A* **1928**, *119*, 173.
(16) Nordhlim, L. W. *Proc. R. Soc. London, Ser. A* **1928**, *121*, 626.
(17) Ding, M.; Kim, H.; Akinwande, A. I. *Appl. Phys. Lett.* **1999**, *75*, 823.
(18) Filip, V.; Nicolaescu, D.; Tanemura, M.; Okuyama, F. *Ultramicroscopy* **2001**, *89*, 39.
(19) Givargizov, E. I.; Zhirnov, V. V.; Stepanova, A. N.; Rakova, E. V.; Kiselev, A. N.; Plekhanov, P. S. *Appl. Surf. Sci.* **1995**, *87*, 24.
(20) Shang, X. F.; Wang, M.; Qu, S. X.; Zhao, P.; Zhou, J. J.; Xu, Y. B.; Tan, M. Q.; Li, Z. H. *Nanotechnology* **2008**, *19*, 065708.
(21) Chen, G.; Wang, W.; Peng, J.; He, C.; Deng, S.; Xu, N.; Li, Z. *Phys. Rev. B* **2007**, *76*, 195412.
(22) Nicolaescu, D.; Hilip, V.; Takaoka, G. H.; Gotoh, Y.; Ishikawa, J. *J. Vac. Sci. Technol. B* **2007**, *25* (2), 472.
(23) Smith, R. C.; Cox, D. C.; Silva, S. R. P. *Appl. Phys. Lett.* **2005**, *87* (10), 103112.
(24) Jeong, S.-H.; Hwang, H.-Y.; Lee, K.-H.; Jeong, Y. *Appl. Phys. Lett.* **2001**, *78* (14), 2052.

AM900490M